JOURNAL OF AIRCRAFT
Vol. 35, No. 2, March–April 1998

Cellular Structures in the Flow over the Flap of a Two-Element Wing

Steven A. Yon* and Joseph Katz†
San Diego State University, San Diego, California 92182-0183

Flow visualization information and time-dependent pressure coefficients were recorded for the flow over a two-element wing. The investigation focused on the stall onset, particularly at a condition where the flow is attached on the main element but separated on the flap. At this condition, spanwise separation cells were visible in the flow over the flap, and time-dependent pressure data were measured along the centerline of the separation cell. The flow visualizations indicated that the spanwise occurrence of the separation cells depends on the flap (and not wing) aspect ratio.

Introduction

SURFACE-FLOW visualization experiments at high angles of attack on rectangular wings showed the existence of organized spanwise cellular patterns, which appear during early poststall condition.[1–3] Those patterns seem to form immediately at the onset of stall and tend to diminish as angle of attack increases. The number of cells depends on wing aspect ratio, with a single-cell aspect ratio of about 1.5–2.5.[2,4] Measurements of the wing surface pressure fluctuations while the above cellular patterns were visible showed that one of the dominant frequencies is much lower[4] than the expected Strouhal frequency of $\omega c/V_\infty = 0.15$. Such information may affect airplane wing design, in view of the fact that the natural vibration modes should not coincide with any anticipated, dominant aerodynamic frequencies. Those considerations are even more pronounced with extended flap systems where the additional flexibility leads to larger vibration levels. Therefore, the main objective of this study is to demonstrate the existence of cellular patterns on the stalled flap during the initial stages of stall; when the flow on the main wing element is still attached. The spanwise spacing of the separation cells is also addressed to determine whether it depends on the whole wing's aspect ratio or on the flap's only. Time-dependent surface pressure variations were measured to provide experimental data for future numerical validations of turbulent separated flows and to determine whether the measured reduced frequency can be scaled based on the whole wing or on the flap chord only.

Experimental Setup

The photograph of the wing as mounted in the wind tunnel is shown in Fig. 1, and its side view is shown in Fig. 2. The main wing plane was kept at zero angle of attack, and the flap angle varied between 30, 35, and 40 deg. Surface tufts were used for flow visualization, and in Fig. 1 two separation cells may be observed. The two-element wing was held by large Plexiglas® end plates to simulate (as closely as possible) two-dimensional flow conditions. The wing, flap, and end-plate assembly was mounted inside a 1.14-m-wide, 0.81-m-tall, 1.66-m-long test section. Additional details on model geometry are presented in Fig. 2. Airspeed was set at V_∞ = 53.6 m/s, resulting in a Reynolds number of 1.28×10^6 based on the wing's combined chord (including the flap). The shape of the main airfoil element is based on the NACA four-digit family, with maximum thickness t/c = 0.18, maximum camber c = 0.12, and location of maximum camber x/c = 0.425 (see Ref. 5, p. 114, on using these values to define the airfoil shape). The flap shape is based on a symmetric NACA 0015 airfoil section. Time-dependent pressure measurements were obtained by small (Endevco 5-mm-diameter, and 1 mm^2 active area) piezoresistive transducers embedded along the flap's chord. The absolute pressure range of the transducers is from 0 to about 1 atm, with a resolution of 0.17×10^{-4} atm and a maximum frequency response of about 0.15 MHz. This accuracy is better than the size of the symbols or thickness of the lines used here to represent the experimental data. The flap section containing the transducers was free to move laterally along the flap span. However, for the present data it was kept at the visual centerline of the left separation cell.

Results

This investigation focused on the condition in which the flow is attached on the main wing element but separated on the flap. Therefore, subsequent to a brief flow visualization experiment to determine the desirable test conditions, the main element orientation was set at zero angle of attack and only the flap angle δ_f varied. Flap stall was observed at δ_f = 40 deg, but at δ_f = 30 deg the flow on the flap was still attached. At this stalled flap condition (δ_f = 40 deg), two stable separation cells were visible on the flap (Fig. 1). Note that all tufts had the same length; therefore, the seemingly longer tufts near the centerline indicate that the flow is attached there, while further out the flow is reversed (the fluttering of the tufts was easily visible during the test, though not entirely captured by the photograph). The aspect ratio of a single separation cell, based on the flap dimensions, is about two, which is close to the values observed on single-element wings.[1,2] Because the wind-tunnel model layout resembled a two-dimensional experiment, one of the widely used two-dimensional airfoil-design codes (MSES)[6] was used for comparison purposes. Results of these computations, in terms of the streamlines near the airfoil and with the measured chordwise pressure distribution, for the two flap deflections are shown in Figs. 3 and 4. The circular symbols represent the time-average pressure coefficient measured on the flap. Both the chordwise positions and the numbering sequence of the transducers are shown on the lower part of Fig. 3. Clearly, at the lower flap deflection the flow is attached (as indicated by the stationary tufts during the flow visualization), and the computed and measured pressures on the flap are satisfactorily close. The computations also show a laminar

Received Feb. 17, 1997; revision received Aug. 26, 1997; accepted for publication Aug. 29, 1997.

*Professor, Department of Aerospace Engineering and Engineering Mechanics. Associate Fellow AIAA.

†Graduate Student, Department of Aerospace Engineering and Engineering Mechanics. Member AIAA.

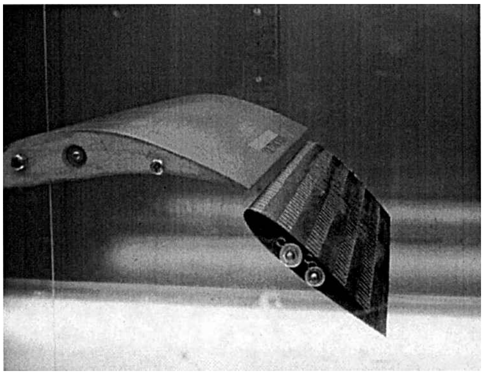

Fig. 1 Two-element wing, as mounted in the wind-tunnel test section. $\delta_f = 40$ deg, and the tufts show two separation cells on the flap.

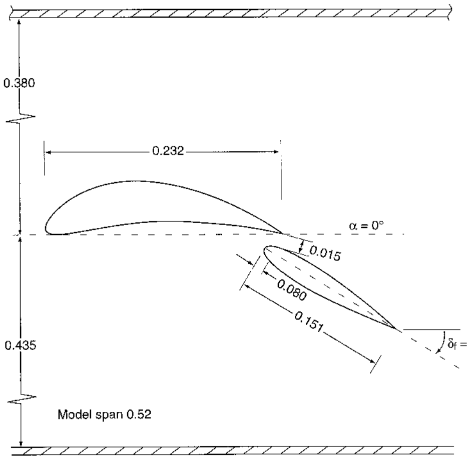

Fig. 2 Geometry of the two-element wing, as mounted in the test section (dimensions in meters).

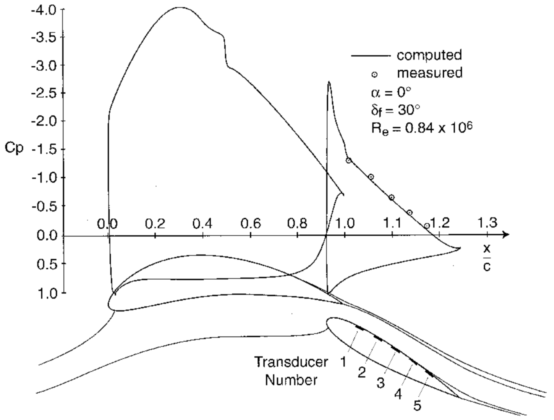

Fig. 3 Computed two-dimensional pressure distribution (using the method in Ref. 6) for the two-element wing at $\delta_f = 30$ deg. The circular symbols show the five measured steady-state flap pressures along the separation cell centerline.

bubble near the midchord of the main element; for such attached-flow conditions the computed results should be close to the actual flow conditions.

Data similar to Fig. 3, but for $\delta_f = 40$ deg, are shown in Fig. 4, where the computed streamlines show an early flow separation on the flap. As mentioned earlier, the flow visualization experiments showed two cellular separation cells on the upper surface (Fig. 1), and the calculated two-dimensional separation point may be viewed as an average representation of the three-dimensional phenomenon. The experimental pressure coefficient data in this figure were measured along the center of the left separation cell and do not compare well with the computed results. The shape of the measured pressure distribution on the flap is quite flat (typical stall), whereas the computations still show a large leading-edge suction. Similar pressure measurements in between the separation cells, but with a single-element wing,[4] showed typical attached-flow pressure distributions with large leading-edge suction. However, the magnitude of the measured data was much smaller than estimated by two-dimensional computations, suggesting an effectively lower angle-of-attack condition there as a result of the downwash created by the adjacent stall cells. Thus, although the test attempts to enforce a two-dimensional condition, the separated flow is naturally time dependent and three dimensional (with significant spanwise variations), and any attempt to compare it with two-dimensional computations may lead to similar discrepancies.

The time-dependent pressure fluctuations, as measured by the five chordwise transducers on the flap, are shown for $\delta_f = 30$ deg in Fig. 5. Note that transducer 1 is closest to the leading edge and transducer 5 is near the trailing edge. The data presented include the time-dependent component only (with an average value of $C_p = 0$), which is obtained by subtracting the time-average value. Similar measurements at $\delta_f = 40$ deg show a large increase in the amplitude of the pressure fluctuations (Fig. 6). The general characteristics of the separated-flow pressure fluctuations in Fig. 6 have a more complicated structure than the quite periodic signal measured with the attached flow

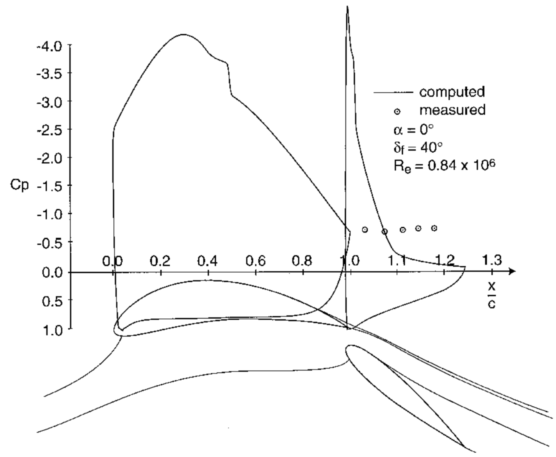

Fig. 4 Computed two-dimensional pressure distribution (using the method in Ref. 6) for the two-element wing at $\delta_f = 40$ deg. The circular symbols show the five measured steady-state flap pressures along the separation cell centerline.

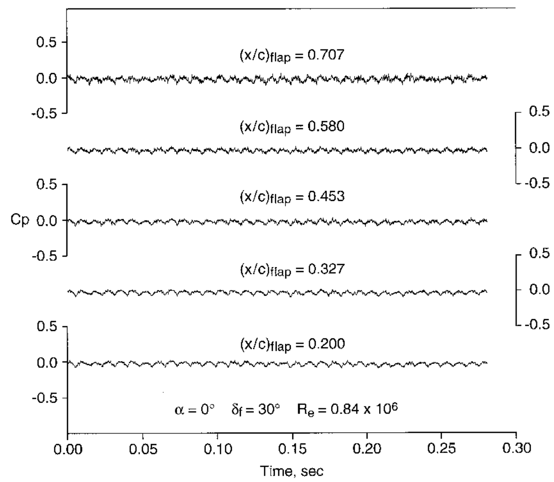

Fig. 5 Time history of pressure coefficients as measured by the five transducers along the flap chord, for $\delta_f = 30$ deg (attached flow). $(x/c)_{\text{flap}}$ is normalized by flap chord, which is about 65% of the main element chord.

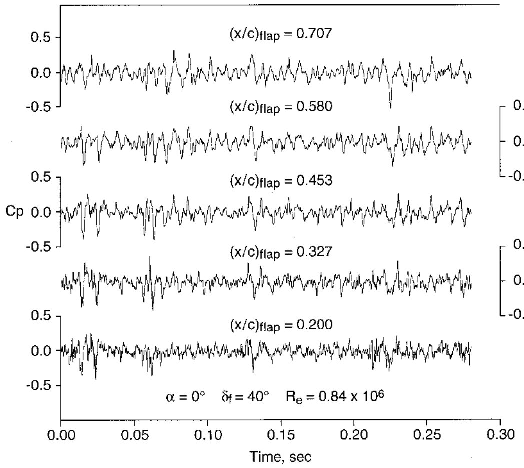

Fig. 6 Time history of pressure coefficients as measured by the five transducers along the flap chord, for $\delta_f = 40$ deg (separated flow).

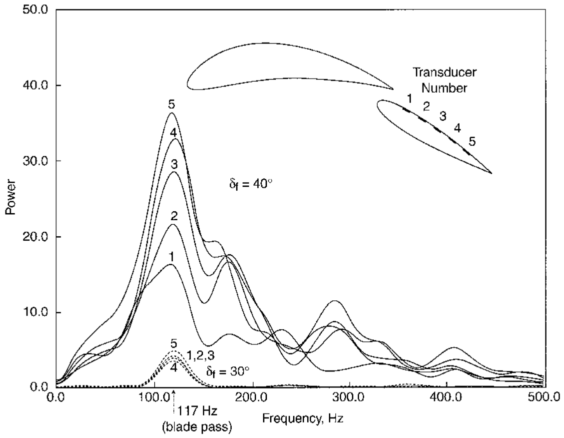

Fig. 7 PSD estimates for the pressure coefficient time histories at $\delta_f = 30$ deg (broken lines) and $\delta_f = 40$ deg (solid lines). Transducer 1 is closer to the leading edge and transducer 5 is near the trailing edge.

(Fig. 5). This observation is true for all five chordwise transducers, and the amplitudes seem to grow toward the flap trailing edge. This growth of the disturbance toward the trailing edge is present in Fig. 5 as well, but at a much smaller magnitude. Having a time-dependent description of the actual small-scale vortices within the separated flow, their structures and transport properties might have determined the source of the preceding fluctuations, but in the absence of such detailed information, the use of some statistical tools may prove useful. Therefore, the power spectra density (PSD) estimates for the time history of the pressure coefficients in Figs. 5 and 6 are shown in Fig. 7. The most dominant frequency is about 117 Hz, and the amplitudes generally increase toward the trailing edge. A closer look at the test facility reveals that the wind-tunnel fan has four blades and rotates at 1750 rpm, which may create a prevalent excitation of about 117 Hz. Figure 7 shows that the power is centered near this driving frequency and that it is considerably amplified in the case of the separated flow. The largest fluctuations in the pressure history in Fig. 6 are clearly responsible for the peak power in Fig. 7 and are caused by the unsteady separated flow, because the baseline (in Fig. 5) contains nothing similar. Cross-correlation between the signals of the individual transducers suggests streamwise convection of the strong periodic component shown in Fig. 6, at about half the freestream velocity. Estimating the Strouhal number based on the frontal height of the separated area of the flap h yields $Sr = \omega h/V_\infty \sim 0.13$, which is quite close to results obtained with single-element wings. Also, in these tests a 50-Hz high-pass filtering was applied to minimize tunnel vibration effects that occur near 30 Hz. Despite this filtering, sizable power under the 50-Hz range is visible for the $\delta_f = 40$-deg case (especially for transducer 1), an effect that is not present at the attached-flow-on-flap case. This indicates that the lower-frequency fluctuations within the separated flow[4,7] are present here as well (but were mostly filtered out by the 50-Hz high-pass filter). Finally, when comparing the power generated in the separated-flow case with the one in the attached-flow case in Fig. 7, the effect of flow separation becomes evident. It seems that the Strouhal-type periodic vortex flow that develops at $\delta_f = 40$ deg causes the sharp increase in the pressure fluctuations. Also, the expected natural frequency of the vortex flow is quite close to the fan-blade passage frequency; similar to the mechanical vibration case, the flow frequency adopts and magnifies the prevailing (forcing) frequency within the freestream. A similar observation is reported in Ref. 4, where the surface pressure fluctuations on a single-element airfoil were recorded; however, the pressure fluctuation frequency measured within the far wake was found to slightly shift toward the natural frequency. Therefore, at this point, it seems that when the driving and natural frequencies are close to each other, the former will dominate the flow near the wing surface. The extension of this rationale to cases with much larger differences between the two frequencies requires additional proof in the form of further experiments.

Conclusions

The presence of spanwise separation cells on the stalled flap of a two-element wing with attached flow on the main element was demonstrated. The cell aspect ratio ($\approx$stall cell span/flap chord) is on the order of two, which is close to the values reported for single-element airfoils. Also, when scaling the dominant pressure fluctuation frequencies observed on the flap, based on the frontal height of the separated area on the flap, the resulting Strouhal number is close to values measured on single-element, stalled wings. When observing the power of the pressure fluctuations in the frequency domain, the frequency of the largest pressure fluctuations, caused by the separated flow, drifted close to the wind-tunnel driving frequency (much like simple mechanical vibrations). This experiment also demonstrates the difficulties of obtaining time-dependent information on the three-dimensional structures within the flow above a wing when using surface information only. Furthermore, real flows are neither two dimensional nor quasisteady, but rather three dimensional and time dependent.

Acknowledgments

This work was funded through NASA Ames Research Center Joint Research Consortium Agreement NCA2-786. James Ross was the Project Monitor.

References

[1]Gregory, N., Quincy, V. G., O'Reilly, C. L., and Hall, D. J., "Progress Report on Observations of Three Dimensional Flow Patterns Obtained During Stall Development on Aerofoils, and on the Problem of Measuring Two-Dimensional Characteristics," Aeronautical Research Council, Fluid Motion Sub-Committee, 31 702, National Physical Lab., Aero Rept. 1309, Jan. 1970.

[2]Winkelmann, A. E., and Barlow, J. B., "Flowfield Model for a Rectangular Planform Wing Beyond Stall," *AIAA Journal,* Vol. 18, No. 8, 1980, pp. 1006–1008.

[3]Weihs, D., and Katz, J., "Cellular Patterns in Poststall Flow over Unswept Wings," *AIAA Journal*, Vol. 21, No. 12, 1983, pp. 1757, 1758.

[4]Yon, S., and Katz, J., "Study of the Unsteady Flow Features on a Stalled Wing," AIAA Paper 97-1927, June 1997.

[5]Abbott, I. H., and von Doenhoff, A. E., *Theory of Wing Sections*, Dover, New York, 1959.

[6]Drela, M., "Design and Optimization Method for Multielement Airfoil Flow," AIAA Paper 93-0969, Feb. 1993.

[7]Zaman, K. M. B. Q., McKinzie, D. J., and Rumsey, C. L., "A Natural Low-Frequency Oscillation of the Flow over an Airfoil Near Stalling Conditions," *Journal of Fluid Mechanics*, Vol. 202, May 1989, pp. 403–442.